Noname manuscript No.
(will be inserted by the editor)

Hao Lu, Christopher J. Rutland

Structural Subgrid-Scale Modeling for Large-Eddy Simulation - A Review

Received July 15th, 2015

Keywords large-eddy simulation, nonlinear, subgrid scale, turbulence

Abstract Accurately modeling nonlinear interactions in turbulence is one of the key challenges for large-eddy simulation of turbulence. In this article, we review recent studies on structural subgrid scale modeling, and the focus is on evaluating how well these models predict the effects of small scales. The article discusses a-priori and a-posteriori test results. Other nonlinear models are briefly discussed, and future prospects are noted.

1 Introduction

Turbulence could dominate all other flow phenomena and result in increased energy dissipation, mixing, heat transfer, and the like. With increased computer power, it is possible to numerically solve governing equations of fluid and obtain a detailed description of a turbulent flow. Direct numerical simulation (DNS) is the most straightforward approach to the solution of turbulence. Recent expansions in computer power have made possible DNS solutions of turbulent flows up to $Re \sim 10^4$ (based on integral scale) [27]. However, most engineering problems concerning fluid dynamics bear much higher Reynolds numbers, and consequently, DNS technology cannot solve the problems [14].

Based on the Reynolds averaging method, Reynolds-averaged Navier-Stokes (RANS) approaches have been the most prevalent way of solving turbulent flows since the 1960s. However, Reynolds-averaging tends to smear out important flow structures in complex flows. Large-eddy simulation (LES), as an alternative approach, solves the large-scale motions of the flow, and models the effects of the smaller universal scales using a subgrid scale (SGS) model [55,46,58]. The main advantage of LES over RANS is the increased level of detail that LES can deliver. With an increase in grid resolution, more flow structures can be resolved in LESs as shown in a growing body of literature [58]. One of the primary reasons for the difference between the two types of approaches is that in comparison to a RANS model, an SGS model usually provides lower dissipation. It is generally accepted that the predictive capability of LES is better than that of RANS in the study of turbulence.

SGS parameterization is considered the most critical part of LES. Numerous SGS models and modeling techniques have been proposed since the introduction of the first SGS stress model by Smagorinsky (1963) [62]. The variety of SGS models has arisen mainly because LES solutions can be sensitive to the models involved. More, users expect that the models involved could adopt fewer adjustable coefficients and be easier to use.

This article will examine the current literature on the development of structural models in incompressible turbulent flows for the sake of simplicity. The existing SGS models developed for incompressible turbulent flows are often applied directly to compressible flow simulations with the usage of Favre filtering [15]. It is assumed, for this article, that the reader is familiar with basic turbulence modeling and has some familiarity with the concepts underlying the LES approach. While some background information is provided, the emphasis is on describing structural LES models.

Hao Lu
School of Energy and Power Engineering, Huazhong University of Science and Technology, Wuhan, China.
E-mail: haolu@hust.edu.cn
Christopher J. Rutland
Engine Research Center, Mechanical Engineering, University of Wisconsin - Madison, Madison, WI, USA.
E-mail: rutland@engr.wisc.edu

2 General LES background

Large-eddy simulation separates resolved and unresolved scales by filtering (with a filter size of Δ) the governing equations of the transport of mass, momentum and scalar quantities. The filtered equations for incompress-

ible flows are

$$\frac{\partial \widetilde{u}_i}{\partial x_i} = 0 \ , \tag{1}$$

$$\frac{\partial \widetilde{u}_i}{\partial t} + \frac{\partial \widetilde{u}_i \widetilde{u}_j}{\partial x_j} = -\frac{\partial \widetilde{p}}{\partial x_i} - \frac{\partial \tau_{ij}}{\partial x_j} + \nu \frac{\partial^2 \widetilde{u}_i}{\partial x_j \partial x_j} + \widetilde{f}_i \ , \tag{2}$$

$$\frac{\partial \widetilde{\theta}}{\partial t} + \widetilde{u}_i \frac{\partial \widetilde{\theta}}{\partial x_i} = -\frac{\partial q_i}{\partial x_i} + \kappa \frac{\partial^2 \widetilde{\theta}}{\partial x_i \partial x_i} \ , \tag{3}$$

where $\widetilde{u}_i$ is the component of the resolved velocity field, $\widetilde{\theta}$ is the resolved scalar, $\widetilde{p}$ is the effective pressure, ν is the kinematic viscosity, κ is the scalar diffusivity, and $\widetilde{f}_i$ is a forcing term (e.g., the buoyancy force, the Coriolis force and other forces). The effects of the subgrid scales on the resolved fields appear in the SGS stress tensor τ_{ij} and the SGS flux vector q_i, respectively,

$$\tau_{ij} = \widetilde{u_i u_j} - \widetilde{u}_i \widetilde{u}_j, \quad \text{and} \quad q_i = \widetilde{u_i \theta} - \widetilde{u}_i \widetilde{\theta}. \tag{4}$$

SGS models are needed to parameterize τ_{ij} and q_i as a function of the resolved velocity and scalar fields.

In general, the SGS term of two arbitrary variables, $\tau_{uv} = \widetilde{uv} - \widetilde{u}\widetilde{v}$, can be decomposed into three components, the Leonard term L_{uv}, the cross term C_{uv}, and the SGS residual term R_{uv}

$$\tau_{uv} = L_{uv} + C_{uv} + R_{uv} \ , \tag{5}$$

where $L_{uv} = \widetilde{\widetilde{u}\widetilde{v}} - \widetilde{\widetilde{u}}\widetilde{\widetilde{v}}$, $C_{uv} = \widetilde{\widetilde{u}v'} + \widetilde{u'\widetilde{v}} - \widetilde{\widetilde{u}}\widetilde{v'} - \widetilde{u'}\widetilde{\widetilde{v}}$, $R_{uv} = \widetilde{u'v'} - \widetilde{u'}\widetilde{v'}$, and the fluctuation of an arbitrary variable is defined as $u' = u - \widetilde{u}$. In addition, with the Gaussian filter, the SGS term can be expanded in the Taylor series [12,55]

$$\tau_{uv} = G_{uv} + O(\Delta^4) \ , \tag{6}$$

where the gradient term is defined as $G_{uv} = \frac{\Delta^2}{12} \frac{\partial \widetilde{u}}{\partial x_i} \frac{\partial \widetilde{v}}{\partial x_i}$. We note that the scalar problem is also a key component of many turbulent flows, and the extension of SGS stress models to scalar flux is not obvious. These two general formulations can also be used for both the SGS stress tensor as well as the SGS scalar flux vector. As will be explained, SGS models can make direct use of the decomposition (5) or the Taylor expansion (6).

A common class of SGS models, eddy-viscosity model and eddy-diffusivity model, parameterizes the SGS stress' deviatoric part and the SGS flux as

$$\tau_{ij} - \frac{1}{3}\delta_{ij}\tau_{kk} = -2\nu_{sgs}\widetilde{S}_{ij}, \quad \text{and} \quad q_i = -\frac{\nu_{sgs}}{Sc_{sgs}} \frac{\partial \widetilde{\theta}}{\partial x_i}, \tag{7}$$

where $\widetilde{S}_{ij} = \frac{1}{2}\left(\frac{\partial \widetilde{u}_i}{\partial x_j} + \frac{\partial \widetilde{u}_j}{\partial x_i}\right)$ is the resolved strain rate tensor, ν_{sgs} is the SGS eddy viscosity and Sc_{sgs} is the SGS Schmidt number. Many models have been used to determine the eddy viscosity. For instance, the Smagorinsky model (SM) [62] computes the eddy viscosity as

$$\nu_{sgs} = (C_S \Delta)^2 \left|\widetilde{S}\right| \ , \tag{8}$$

where $\left|\widetilde{S}\right| = \left(2\widetilde{S}_{ij}\widetilde{S}_{ij}\right)^{\frac{1}{2}}$ is the strain rate, and C_S is the Smagorinsky coefficient. By assuming a local equilibrium between production and dissipation of SGS kinetic energy, analyses in isotropic turbulence show $C_s \approx 0.17$ and $Sc_{sgs} \approx 0.5$ [33,1]. However, flow anisotropy, for instance, the presence of a strong mean shear near the surface in high-Reynolds-number atmospheric boundary layers (ABL) makes the optimum values of those coefficients depart from their isotropic counterparts [6]. Using dynamic procedure [16], Piomelli (1993) [51] has shown that $(C_S\Delta)^2$ displays a $(y^+)^3$ power-law behavior near the bounded-wall.

The eddy-viscosity/diffusivity models assume that the effects of SGS motions on resolved scales are essentially energetic actions, and that the energy-transfer mechanism is analogous to the molecular mechanism represented by diffusion. The models use the same eddy-viscosity or eddy-diffusivity for all directions, which is not accurate for anisotropic turbulence. Also, the local-equilibrium hypothesis is usually adopted to determine the model coefficients. Studies [12,42] have shown that the modeled SGS terms correlate poorly with the corresponding exact SGS terms. In LES using these models, kinetic energy can transfer only from resolved to unresolved scales. For numerical stability, this is a desirable characteristic. However, in anisotropic turbulence, there can exist a net transfer of kinetic energy from small to large scales [7, 63]. The SGS motions might also facilitate kinetic energy transfer from unresolved to resolved scales in a process referred to as "backscatter." An important feature of good SGS models is that they can let the nonlinear interactions occur while still maintaining numerical stability. Figure 1 shows the power spectra of the kinetic energy transfer term between the resolved and unresolved scales obtained using several models. Structural models follow the spectra from the DNS results much better than two eddy-viscosity models. In contrast, two eddy-viscosity models show high values at all wavenumbers, indicating that they take excessive energy out of the resolved scales and reduce the possibility of nonlinear interactions occurring at large scales (low wavenumbers). In addition, we note that the excessive dissipation delivered by the SM can have negative impacts on the turbulent flow. For instance, time correlation is critically important to turbulence-generated noise and particle-laden turbulence, it has been found that the SM over-predicts time correlation and increases the length scales of LES fields in either space or time [19,20,74,26].

The eddy-viscosity/diffusivity models primarily focus on the balance of the energy transfer between resolved and unresolved scales. In a different manner, the structural SGS modeling focuses on predicting the exact SGS term by a direct reconstruction (usually on the basis of its Taylor expansion or decomposition), and requires no knowledge of the inter-scale interaction. Clark et al (1979) [12] derived the first structural model from the

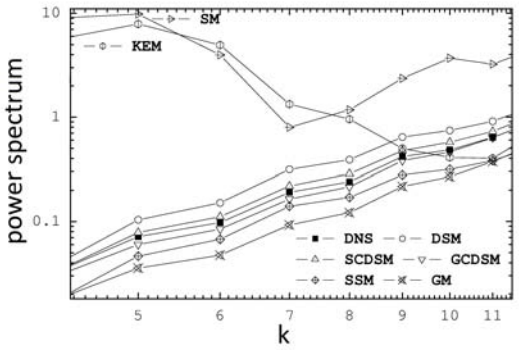

Fig. 1 Power spectra of the SGS kinetic energy production as a function of wavenumber for a rotating turbulence. DNS stands for direct numerical simulation; SM stands for Smagorinsky model; KEM stands for viscosity-based kinetic energy equation model; SSM stands scale-similarity model; GM stands gradient model; and the rest are variations of the dynamic structure model. Figure is a modified version of figure 20 in Lu et al 2007 [42].

Taylor expansion of the SGS stress tensor, and one year later, Bardina et al (1980) [4] were the first to introduce a similarity type structural model. There is a broad perception that structural modeling is an improvement over eddy-viscosity/diffusivity modeling:

1. structural models serve to reconstruct SGS information by using resolved fields;
2. structural models do not locally assume the same eddy-viscosity or eddy-diffusivity for all directions;
3. structural models do not assume that the small scales always drain energy from the large scales, and can predict the exact SGS terms more accurately than eddy-viscosity/diffusivity models; hence, they could improve the capturing of anisotropic effects and the prediction of energy transfer and disequilibrium;
4. similarity type structural models are based on a scale-invariance assumption, which is fairly well satisfied in turbulent flows;
5. gradient type structural models use velocity gradients and scalar gradients to complete the modeling, and, thus, can be extremely computationally efficient as the standard eddy-viscosity/diffusivity models.

These features make structural models attractive.

3 Algebraic structural model

The most straightforward method for structural modeling involves the use of equations (5) and (6). The gradient model (GM), which was first derived by Clark et al (1979) [12], can be written as

$$\tau_{ij} = G_{u_i u_j} \ , \quad \text{and} \quad q_i = G_{u_i \theta} \ , \tag{9}$$

and the scale-similarity model (SSM), which was first introduced by Bardina et al (1980) [4], can be written as

$$\tau_{ij} = L_{u_i u_j} \ , \quad \text{and} \quad q_i = L_{u_i \theta} \ . \tag{10}$$

In the literature, there are some variations on the model formation of the GM and the SSM, but they have common basic characteristics.

However, when implemented in actual LESs, the two basic models are often unable to predict the correct levels of SGS energy production, and as a result, simulations become numerically unstable as reported in a variety of contexts [55,58]. Motivated by a dynamic structure model (DSM) introduced by Pomraning and Rutland (2002) [54], Lu and Porté-Agel [38,37,39,40] proposed a modulated gradient model (MGM) formulation to resolve the numerical stability issue. The algebraic nonlinear closure for the SGS stress tensor and for the SGS flux vector can be formatted as

$$\tau_{ij} = 2k_{sgs} \left(\frac{G_{u_i u_j}}{G_{u_k u_k}} \right) \ , \text{ and } \ q_i = |\mathbf{q}| \left(\frac{G_{u_i \theta}}{|G_{u_i \theta}|} \right) \ . \tag{11}$$

The closure separates the modeling into two elements: the normalized gradient term serves to model the structure (the relative magnitude of each component); and a separate proced is needed for the magnitudes.

In an algebraic closure [38,37,39], one can evaluate the value of k_{sgs} on the basis of the local equilibrium hypothesis, which assumes a balance between the SGS production and the dissipation rate. The SGS kinetic energy production is defined as $P = -\tau_{ij} \frac{\partial \widetilde{u}_i}{\partial x_j}$, and a classical evaluation of the kinetic energy dissipation rate is $\varepsilon = C_\varepsilon \frac{k_{sgs}^{3/2}}{\Delta}$. More, the SGS scalar variance production is defined as $P_\theta = -q_i \frac{\partial \widetilde{\theta}}{\partial x_i}$, and a classical evaluation of the SGS scalar variance dissipation rate is $\varepsilon_\theta = C_{\varepsilon\theta} \frac{\theta_{sgs}^2 u_{sgs}}{\Delta}$, where $\theta_{sgs} = |\mathbf{q}|/u_{sgs}$ and $u_{sgs} = \sqrt{2k_{sgs}}$. The closure uses only local velocity and scalar gradients, and it does not require an extra filtering. These features make the closure computationally efficient. The computational cost using this closure is similar to the standard eddy-viscosity/diffusivity models, however, it gives much less SGS dissipation and yields better small-scale statistics (which can been shown by means of spectra [38,37,39]). This algebraic structural closure is probably the simplest structural approach to achieve stable LESs. It has shown excellent results in wind-turbine simulations [60] and LES of idealized urban flows [8,9], and has motivated several recent modeling studies (e.g., [40,17,18]).

There exist two SGS model coefficients in this algebraic structural closure, C_ε and $C_{\varepsilon\theta}$. One can use classical values obtained from turbulence statistics, and another method for computing the two coefficients is to apply the so-called dynamic procedure, which is based on the Germano identities [16,34] for the SGS stress tensor and the SGS flux vector. The dynamic procedure is

very useful and can be used for many models to find optimized modeling coefficients. Lu and Porté-Agel (2014) [40] have shown that, in simulations of ABL flows, the dynamic version of the MGM yields results that are more accurate than the results yielded by using two constant coefficients. This research finding strongly suggest that the aforementioned dynamic model is an excellent choice for LES applications (e.g., [41]). Recently, Ghaisas and Frankel (2015) [18] evaluated several dynamic versions of the gradient-type structural SGS stress model and SGS flux model. Accurate first-order and second-order turbulent statistics confirm that the MGM kernel is suitable for the use with the global-dynamic procedure in LESs of neutral and stably stratified channel flows.

Regarding the development of the SGS scalar flux model, Balarac et al (2013) [2] proposed a regularization of the gradient model by neglecting the stretching effects in the model formulation. A physical interpretation of this regularization is that the stretching effect leads to "backscatter" (involving negative value of SGS dissipation) and causes numerical instabilities. So, their assumption logically results in the removal of the part causing "backscatter," and this method is similar to the clipping procedure used for the modulated gradient SGS flux model proposed by Lu and Porté-Agel (2013) [39]. The dynamic version of this regularized gradient model provides a better prediction of scalar variance transfers than the GM, and shows, in both a-priori and a-posteriori test levels, a substantial improvement for various scalar statistics predictions. To improve the accuracy of flux magnitude modeling, Ghaisas and Frankel (2014) [17] introduced four flux models. The normalized gradient term, $\left(\frac{G_{u_i\theta}}{|G_{u_i\theta}|}\right)$, and the normalized Leonard term, $\left(\frac{L_{u_i\theta}}{|L_{u_i\theta}|}\right)$, serve to model the structure of the SGS scalar flux vector with the aim of maintaining good orientations between the exact and the model SGS flux vectors. Their proposed SGS flux model have been evaluated in LESs of channel flows, and show promising performances [18].

Another method for resolving the issue of instability is to include a model for the residual part, R_{uv}, which can be used to stabilize the simulation. It is quite common to use a linear combination of a structural model and an eddy viscosity model for the SGS stress tensor

$$\tau_{ij} = L_{u_iu_j} - 2\nu^m_{sgs}\widetilde{S}_{ij}, \text{or } \tau_{ij} = G_{u_iu_j} - 2\nu^m_{sgs}\widetilde{S}_{ij}. \quad (12)$$

To determine the model coefficient for the SGS viscosity, one can use quite a few methods [77,69], including the dynamic procedure [16]. Mixed models combine the strengths of structural models and eddy-viscosity models. This approach has been proven a great success in many turbulent flows, such as the flows of a lid-driven cavity [77], a mixing layer [70], and rotating turbulence [30,42,43]. It must be noted that the viscosity term does not degrade the a-priori results, because typically the magnitude of a structural term in the noted models is significantly higher than that of the viscosity term [36]. Note here that, in order to overcome traditional eddy viscosity's excessive dissipativeness at large scales, which may hinder energy from transferring to large scales, research has suggested [5,13] that the LES community should consider a hyper viscosity that can model the residual SGS term. For instance,

$$\tau_{ij} = G_{u_iu_j} + \nu^u_{sgs}\nabla^2\widetilde{S}_{ij}. \quad (13)$$

Also, to overcome the problem that the Leonard term, L_{uv}, is not material-frame-indifference consistent with the exact SGS term, one can use a model for the cross term, C_{uv}, to get better models [42,43].

4 One-equation structural model

The local equilibrium hypothesis relies on a sufficiently large statistical sample that usually does not exist at the SGS level in a complex flow. Also, it has been observed [17] that the simple algebraic model described in equation (11) may not be able to provide a good approximation for the SGS kinetic energy, k_{sgs}. Alternative methods to compute k_{sgs} are needed.

A one-equation LES model was developed and widely used for ABL flows [59,47], and probably, the first useful one-equation model for engineering flows was introduced by Kim and Menon (1995) [29]. Sone and Menon (2003) [64] applied the one-equation model to engine applications and had good results. One-equation model solves the transport equation of the SGS kinetic energy

$$\frac{\partial k_{sgs}}{\partial t} + \widetilde{u}_j\frac{\partial k_{sgs}}{\partial x_j} = -\tau_{ij}\frac{\partial \widetilde{u}_i}{\partial x_j} - C_c\frac{k^{3/2}_{sgs}}{\Delta} + \frac{\partial}{\partial x_j}\left[\left(\frac{\nu_{sgs}}{\sigma_k} + \nu\right)\frac{\partial k_{sgs}}{\partial x_j}\right], \quad (14)$$

where, $\nu_{sgs} = C_k\sqrt{k_{sgs}}\Delta$, and the three terms on the right-hand side represent, respectively, the production, the dissipation, and the diffusion of the SGS kinetic energy. The typical values for the constants are $C_k = 0.05$, $C_c = 1.0$ and $\sigma_k = 1.0$ [76].

In comparison to the algebraic approach, the use of this transport equation has several distinct features:

1. it relaxes the assumption of local balance between the SGS kinetic energy production and the dissipation rate;
2. it incorporates more physical processes including the convection, production and dissipation of k_{sgs};
3. it requires only one major modeled term, the dissipation of k_{sgs}, which represents the fairly universal energy transfer below the subgrid scales and can be quite accurately modeled using simple models, e.g., $C_c\frac{k^{3/2}_{sgs}}{\Delta}$ in Eqn. (14);
4. it makes the accuracy of SGS stress modeling better than the accuracy of other eddy-viscosity models;

5. it provides velocity scaling, $u_{sgs} = \sqrt{2k_{sgs}}$, that can be used for a scalar flux model, a combustion model, a spray model, and so on.

Most one-equation models adopt k_{sgs} to predict the SGS eddy viscosity, ν_{sgs}, to close Eqn. (7); nevertheless, one-equation structural model adopts k_{sgs} to predict the magnitude of the SGS stress tensor as shown in Eqn. (11). Pomraning and Rutland (2002) [54] and Chumakov and Rutland (2005) [11] introduced DSMs to LES turbulence modeling. Their models are written as

$$\tau_{ij} = 2k_{sgs}\left(\frac{L_{u_i u_j}}{L_{u_k u_k}}\right) , \quad \text{and} \quad q_i = \left(\frac{\Theta}{L_{\theta\theta}}\right) L_{u_i\theta} , \quad (15)$$

where Θ is the SGS scalar variance. This structural closure has been developed at University of Wisconsin - Madison for practical applications, especially internal combustion engines, and has been proved to be a good approach in combustion, scalar mixing and spray modeling [25,22,23,3]. In recent LES studies on rotating turbulence [43], a hyper-viscosity mixed version of the gradient-type dynamic structure model,

$$\tau_{ij} = 2k_{sgs}\left(\frac{G_{u_i u_j}}{G_{u_k u_k}}\right) + \nu^u_{sgs}\nabla^2\widetilde{S}_{ij} , \quad (16)$$

has also yielded good results. It is also very computationally efficient because the implementation of the gradient-type models does not require test filtering.

5 Testing structural models

In this section, we present a-priori results and a-posteriori results regarding structural models.

5.1 A-priori test

An a-priori test [12,52] is a fundamental approach to directly comparing exact SGS terms and modeled SGS terms. This comparison serves as a standard testing technique for SGS models, and helps to reveal which models capture more details of an SGS field and which models though designed to capture average behavior may miss details. The a-priori test requires data that have a high spatial resolution sufficiently resolving the SGS range. One can use PIV measurements [35] or DNS data [42]. Figure 2 presents an example of a qualitative a-priori evaluation involving comparisons of representative contour plots of τ_{11} calculated in an isotropic flow using the SSM and a filtered DNS data [42]. The SSM uses the assumption of scale invariance in a strong sense. As summarized by Meneveau and Katz (2000) [46], the full structure of the velocity field at subgrid scales is postulated to be similar to that at resolved scales. Therefore, the SSM can duplicate much of the general structure of the SGS stress.

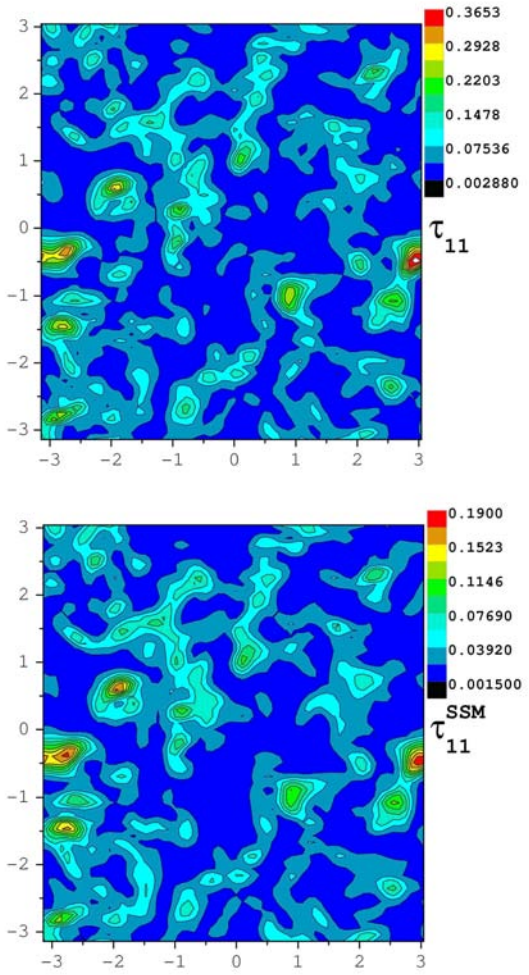

Fig. 2 Contour plots of the exact SGS stress τ_{11} (up) and the scale-similarity modeled stress τ_{11}^{SSM} (down) in a 128^3 isotropic turbulent case. The cut-off wavenumber of the Gaussian filtering for the SSM is $k_c = 32$. Figure is a modified version of figure 9 in Lu et al 2007 [42].

More quantitative a-priori evaluations can be made on the basis of turbulence statistics (e.g., mean field profiles, turbulence intensities) [52], probability density functions [11,10,42], scatter plots [35,46,11,42], orientation [17], and so on. Clark et al (1979) [12] have used the correlation coefficient to quantitatively evaluate various SGS models. The range of the correlation coefficient is -1 to 1. However, negative values of the correlation coefficient rarely occur in LES a-priori testing and values close to 1 indicate a strong correlation. To better reveal the overall accuracy of modeling, Lu et al (2007) [42] suggested another coefficient, the regression coefficient. A departure from 1 in the regression indicates a loss of ability to capture the correct magnitude level of resolved flow quantities. As shown in Figure 2, the similarity of two contour plots can be evaluated using the correlation coefficient (about 0.94), and the magnitude difference of

the contour levels can be evaluated using the regression coefficient (about 0.52).

The eddy-viscosity model rests on the assumption of a one-to-one correlation between the SGS stress tensor and the strain rate tensor. It has been found that the strain rate tensor has a low correlation level (< 0.4) with stress components [12,42]. In particular, Lu et al (2007) [42] showed that in rotating turbulence, the SM yields very low correlation coefficients (< 0.03) for stress components, and a one-equation eddy-viscosity yields a low-correlation level (about 0.3) on cross terms. In contrast, structural models based on the SSM or the GM usually yield high correlation coefficients (> 0.7) in a-priori tests, indicating that the models can capture the flow structure better than the eddy-viscosity models.

Detailed a-priori tests of SGS scalar flux models have also been performed in recent years. Ghaisas and Frankel (2014) [17] have performed a-priori analyzes of various SGS flux models by using DNS data of passive and active scalars. Using correlation coefficient and regression coefficient as their primary tools, they have found that dynamics structure models are excellent at predicting the structure and the magnitude of exact SGS fluxes, and have also found their four proposed structural models yield improvements on the prediction of the magnitude of SGS fluxes.

5.2 A-posteriori test

Certain risks can arise if an investigation of the model performance in actual LES of turbulent flows had not been performed. A-priori results of the GM are superior to those of eddy-viscosity models; however, the GM does not provide sufficient dissipations at small scales [4]. For this reason, a-posteriori test, named by Piomelli et al (1990) [53], is considered an ultimate test of an SGS model.

One of the earliest examples of a-posteriori test of structural models was performed in the mixing layer by Vreman et al (1997) [70]. Their research examined the evolution of resolved kinetic energy and presented evidence that the SM yields excessive dissipation of energy in the transitional regime of the simulation so that the transition to turbulence is hindered. The results using the dynamic SM suggests that, in general, the dynamic procedure not only can be used to determine the model coefficient, but also can resolve the major shortcoming of the SM, namely the excessive dissipation in the transitional regime. The GM appears to offer no improvement over the no-model simulation. It is interesting to see that in the mixing layer, the SSM dissipates approximately the correct amount of energy. Two dynamic mixed structural models accurately predict the evolution of the total kinetic energy, and the dynamic similarity-type mixed model yields results that are most close to the filtered DNS data.

Chumakov and Rutland (2005) [11] tested the DSM and the one-equation eddy-viscosity model in decaying isotropic turbulence. The differences between the performance of two models can be clearly demonstrated in figure 3, which shows the evolution of the fraction of the total kinetic energy stored in the unresolved scales. The final period of the decay is characterized by the absence of the inertial range thus the SGS kinetic energy part should decrease rapidly to zero as the decay approaches the final period. It is clear that the DSM captures the expected behavior well; while, LES using the one-equation eddy-viscosity model leaves from 5 to 10% of the total kinetic energy in the unresolved scales at all times.

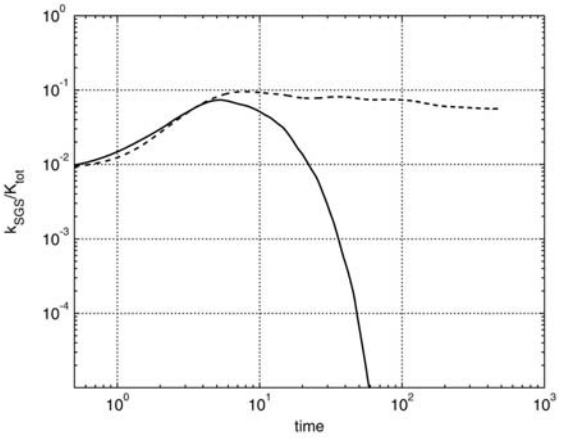

Fig. 3 Comparison of the evolution of k_{sgs}/k_{total} in decaying isotropic turbulence. The solid line refers results obtained using the dynamic structure model, the dashed line refers results obtained using one-equation eddy-viscosity model (from Chumakov and Rutland 2005 [11], Fig. 7. reprinted with permission from John Wiley and Sons).

Lu and Porté-Agel (2010, 2013, 2014) [38–40] studied the model performance of the algebraic structural closure (Eqn. (11)) in high-Reynolds-number turbulent ABL flows. The ABL flow bears a wide range of turbulent length scales, from millimeters to kilometers, and is considered one of the most difficult types of turbulent flows to simulate owing to the complex physical processes involved in ABL flows. Figure 4 shows that the standard eddy-viscosity/diffusivity models yield unrealistic mean velocity and scalar profiles, with excessive non-dimensional mean shear and scalar gradients. The models are too dissipative (which can also been shown by means of spectra [56]), and they remove too much kinetic energy from the resolved field and generate near-linear profiles in the surface layer, which bear large values of Φ_M and Φ_θ. In contrast, the algebraic structural closure delivers significant improvement and yields the value of Φ_M which remains close to 1 (indicative of the expected logarithmic velocity profile), and the value of Φ_θ which remains close to 0.74. The satisfactory results

in ABL flows have shown that: (1) the standard GM, when properly modified, can achieve stable and robust simulations, (2) the local equilibrium hypothesis together with a simple clipping procedure may provide an estimation of the SGS kinetic energy for the model, and (3) the application of the algebraic structural closure to ABL flows shows that the structural approach can achieve the expected logarithmic velocity profile in the near-wall region, the correct spectral scaling, as well as other important statistical characteristics of ABL.

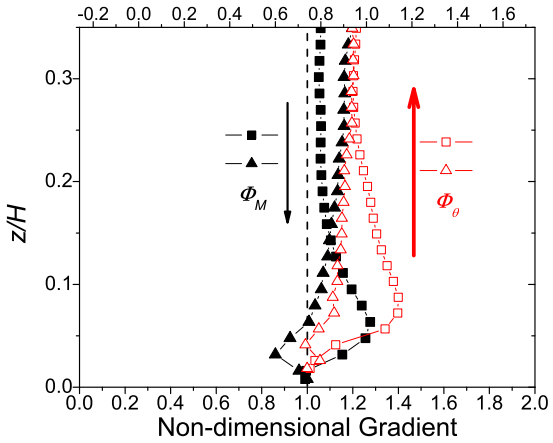

Fig. 4 Nondimensional vertical gradients of the mean resolved streamwise velocity and temperature. ■ and □ correspond to results obtained through the use of standard eddy-viscosity/diffusivity model with *ad-hoc* damping; ▲ and △ correspond to results obtained through the use of the algebraic structural closure shown in equation (11); the dashed line corresponds to the classical similarity profile. Figure is a modified version of figures from Lu and Porté-Agel 2010, 2013 [38,39].

In convective ABL flows, the warmer land surface leads to an upward heat flux, which creates thermal instability. Vertical-velocity skewness is indicative of the structure of the motion, and a positive value of the skewness means that updrafts are narrower than surrounding downdrafts. Studies have found a number of puzzling features of the vertical-velocity skewness in LESs. Figure 5 presents the normalized vertical-velocity skewness of convective ABL flows obtained from LESs using two eddy-viscosity/diffusivity closures [49,45,48] and the dynamic version of the algebraic structural closure [40,41], the Minnesota experiment data [73], and AMTEX field measurement data [32]. There is good agreement over the lower part of the convective ABL; however in the upper part, LESs using eddy-viscosity models [49,45,48] predict a further increase in the vertical-velocity skewness, while actual observations point to a nearly constant value. Simulation results in a convective ABL obtained using the structural closure [41] evidently show much more accurate vertical-velocity skewness predictions.

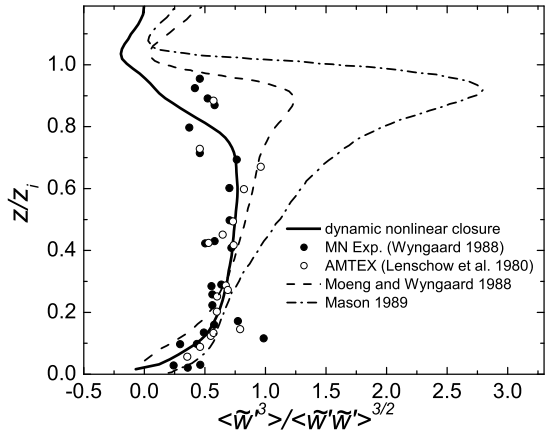

Fig. 5 Vertical-velocity skewness profile in convective ABL. The solid line stands for LES results using the dynamic version of the closure presented in equation (11) [40]; • stands for Minnesota experiment data; ○ stands for AMTEX field measurement data; the dashed line stands for LES results from Moeng and Wyngaard, 1988 [49]; the dashed-dotted line stands for LES results from Mason 1989 [45].

In the tests of the structural flux models, Balarac et al (2013) [2] examined the time evolution of LES resolved scalar variance in isotropic turbulence. The dynamic eddy-diffusivity model always yields notably smaller resolved scalar variance than the filtered DNS. The primary reason is the model's over-prediction of the SGS dissipation, which is also found in their a-priori tests. The GM resolved scalar variance is higher than the DNS scalar variance. Their proposed structural flux model, the dynamic regularized gradient model, corrects this problem and delivers results that are mostly close to the filtered scalar variance.

One of the important features of LES is that it can capture large-scale coherent structures better than RANS, and with an increase in grid resolution, LES can resolve more details of turbulent flows than RANS. Particularly in a reacting flow, LES is considered a more useful method for understanding the flow physics and also for undertaking industrial design [57]. However, an important issue that has received little attention is how SGS models affect coherent structures. Vreman et al (1997) [70] have shown that different models can lead to qualitative differences in the coherent structure of a mixing layer, and that the mixed structural models yield better results than other traditional models.

Further, recent research has investigated models' ability to capture large-scale structures in rotating turbulence. Rotating turbulence provides a simple configuration for studying the characteristic features and model performances in anisotropic turbulent flows. The Coriolis force appears in the momentum equations as a linear part; however, it may radically change the nonlinear dynamics. It is well known that rotation has a significant influence on large-scale atmospheric and oceanic

flows as well as on some engineering flows (e.g., turbulence in jet engines). Studies [7,63] have addressed that rotation turbulence can yield a tendency toward 2D flow, a cyclonic/anti-cyclonic asymmetry in favor of cyclones, reduced kinetic energy transfer from large to small scales, and reverse energy transfer from small to large scales. To deliver these features, accurate modeling of the effects of rotation on turbulence using LES can be a great challenge. Probability density function (PDF) of ω_3 in figure 6 shows that a mixed one-equation structural model can capture the cyclonic/anti-cyclonic asymmetry in an intermediate-scale forced LES of rotating turbulence while other standard SGS models, especially eddy-viscosity models, fail to do so. Lu et al (2008) [43] have also presented evidence that the structural model can provide sufficient dissipation of kinetic energy at small scales and can capture reverse energy transfers to large scales (Fig. 7). However, eddy-viscosity models are by construction fully dissipative, and do not allow for reverse energy transfers. The mergence of the 2D and 3D kinetic-energy spectra in the energy-containing range shown in Fig. 7 is also a demonstration of the tendency toward 2D flows, with much lower levels of kinetic energy in the velocity component parallel to the rotation axis.

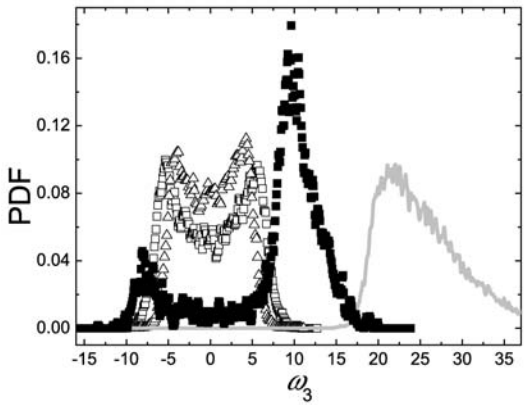

Fig. 6 PDF of ω_3 obtained from the filtered DNS (gray line), the Smagorinsky model (△), a mixed scale-similarity model (□) and a mixed one-equation structural model (■). Figure is a modified version of figure 10b in Lu et al 2008 [43].

In recent years, LES has been applied in practical internal combustion engine simulations. One of the challenges for this type of simulation is accurate modeling of a liquid fuel injection process characterized by high injection pressure, small nozzle hole size compared to engine cylinder size (wide range of length scales), and two-phase compressible flow. A good SGS model is required to correctly capture the large scale and sub-grid interactions with liquid droplets. Tsang et al. (2014) [68] studied the performance of three different SGS models in a constant-volume evaporating Diesel fuel spray. The experimental data can be found in at the Engine Combustion Network website [72]. The three SGS models are the Smagorinsky, a one-equation viscosity-based model, and the dynamic structure model. The dynamic structure model was modified to account for high injection pressure of Diesel sprays. Artificial viscosity was added in the near-nozzle region where the strain rate is high. That is, in this region a mixed model (dynamic structure + viscosity-based) is used. The purpose of adding this term is to enhance sub-grid mixing in the near-nozzle region. Three different grid sizes, 1.0 mm, 0.5 mm, and 0.25 mm, were tested. Note that the smallest grid size, 0.25 mm, is still larger than the nozzle hole size, 0.09 mm. Under this level of mesh resolution the expectation is that a good SGS model should predict correct global quantities such as liquid and vapor penetrations and overall spray plume shape. Figure 8 shows the temperature contours predicted by the three SGS models using the 0.25 mm mesh. Compared to the experimental image, the dynamic structure model gives the best prediction in terms of jet spreading. The Smagorinsky model gives fairly good prediction but narrower spray shape compared to the experimental image. The contour predicted by the one-equation viscosity-based model is much narrower and no flow structures can be observed. Tsang et al. (2014) [68] found that the magnitude of SGS eddy-viscosity predicted by the one-equation viscosity-based model is about three to four times larger than that predicted by the Smagorinsky model, resulting in over-damping. Figure 9 shows liquid and vapor penetrations predicted by the three models in different mesh resolutions. Vapor penetration results predicted by the dynamic structure model converge to experimental data when the grid size is smaller than or equal to 0.5 mm. The Smagorinsky model gives fairly good prediction of vapor penetration at later times for the 0.25 mm and 0.5 mm mesh, but it over predicts vapor penetration at early times. The one-equation viscosity-based model fails to give reasonable prediction of vapor penetration. From

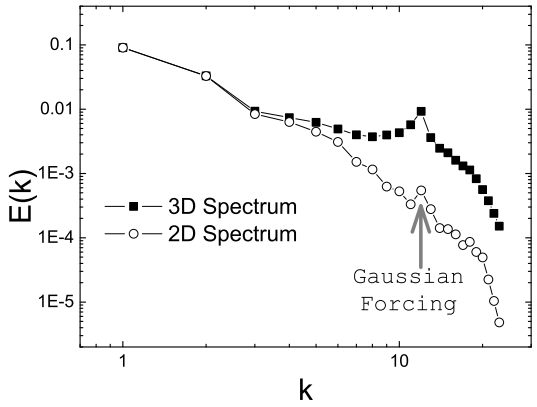

Fig. 7 3D & 2D kinetic energy spectra obtained from a mixed one-equation structural model. Figure is a modified version of figure 10a in Lu et al 2008 [43].

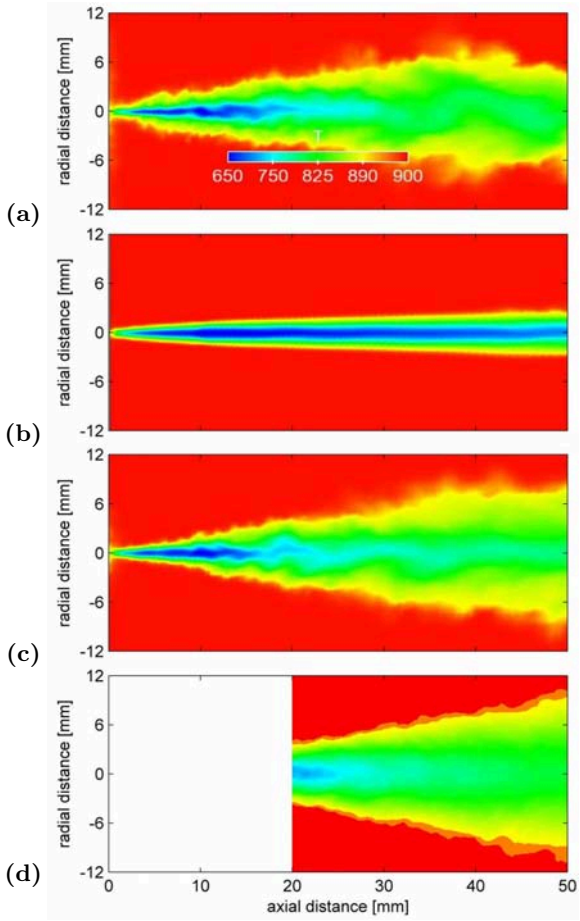

Fig. 8 Comparisons of the instantaneous temperature contours at 2.0 [ms] for the 0.25 [mm] mesh predicted by the (a) the Smagorinsky model, (b) the one-equation viscosity-based model, and (c) the dynamic structure model, respectively. The ensemble-averaged temperature contour measured by the ECN experiment is shown in (d). Figure is from Tsang et al. 2014 [68], Fig. 11, reprinted with permission from Elsevier.

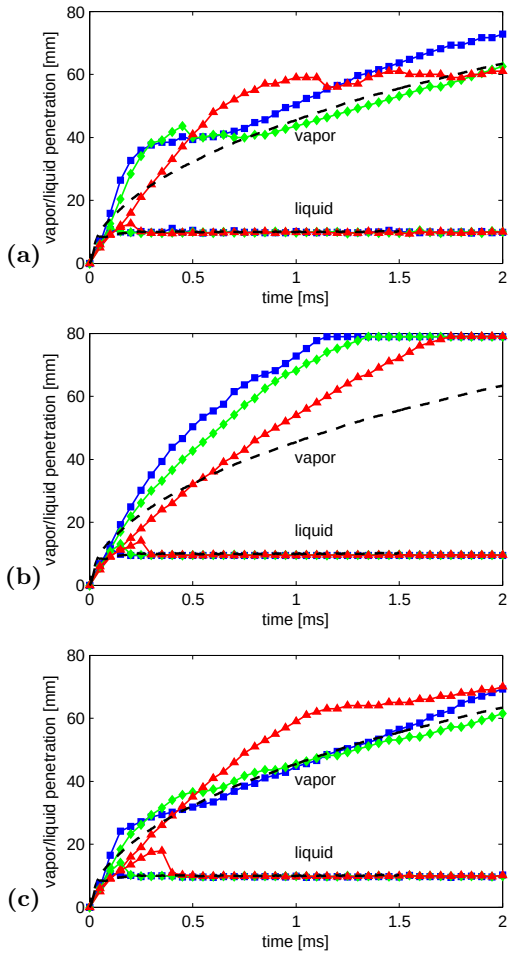

Fig. 9 Vapor and liquid penetrations predicted by the (a) Smagorinsky model, (b) one-equation model, and (c) dynamic structure model using the 0.25 [mm] mesh, the 0.5 [mm] mesh, and the 1 [mm] mesh. The black dashed line shows the ECN experiment data. Figure is from Tsang et al. 2014 [68], Fig. 15, reprinted with permission from Elsevier.

this study, we can see that these three SGS models gave distinct predictions. They also examined the temperature contours predicted by the 0.5 mm mesh and the 1 mm mesh. Under these two coarser mesh resolutions, only the dynamic structure model can predict reasonable jet spreading. The conclusion is that the dynamic structure model is the best compared to the other two viscosity-based models, and it is less sensitive to grid resolution. This may correspond to the more correct prediction of power spectra of the SGS kinetic energy production as shown in figure 1.

6 Other nonlinear SGS stress models

Nonlinear SGS stress models have also been proposed independently of the GM and the SSM. Research conducted by Lund and Novikov (1992) [44] is some of the earliest example to use tensor theory [78,24] in order to study nonlinear combinations of filtered velocity gradients at a-priori test level. Unfortunately, the aforementioned study did not find significant improvements over the SM as the number of terms is increased. Later, Kosović (1997) [31] proposed a nonlinear model for ABL flow

$$\tau_{ij} = -2\nu_{sgs}\widetilde{S}_{ij} + c_1\Delta^2\widetilde{S}_{ik}\widetilde{S}_{kj} + c_2\Delta^2\left(\widetilde{\Omega}_{ik}\widetilde{S}_{kj} - \widetilde{S}_{ik}\widetilde{\Omega}_{kj}\right), \quad (17)$$

where $\widetilde{\Omega}_{ij} = \frac{1}{2}\left(\frac{\partial\widetilde{u}_i}{\partial x_j} - \frac{\partial\widetilde{u}_j}{\partial x_i}\right)$ is the antisymmetric part of the resolved velocity gradient tensor. Applications of this model to the LES of ABL flows yield improvements over the eddy-viscosity models. As pointed out by Horiuti (2003) [21], Kosović's original derivation [31] suffered

from a problem regarding the sign of one model coefficient, and it would disrupt the transformation of the flat sheet structure into the vortex tube. The problem was corrected in Kosović's later simulations [50] and in simulations by other researchers [75]. Wang and Bergstrom (2005) [71] have also introduced nonlinear models that use the symmetric and antisymmetric parts of the resolved velocity gradients. In the numerical simulations of turbulent Couette flows at modulated Reynolds numbers, their models can boast many capabilities that the standard eddy-viscosity models cannot.

The general form of the nonlinear SGS stress models can be written as [66]

$$\tau_{ij} = \alpha_1 l^2 \widetilde{S}_{ik}\widetilde{S}_{kj} + \alpha_2 l^2 \left(\widetilde{S}_{ik}\widetilde{\Omega}_{kj} - \widetilde{\Omega}_{ik}\widetilde{S}_{kj}\right) + \alpha_3 l^2 \widetilde{\Omega}_{ik}\widetilde{\Omega}_{kj} \ , \quad (18)$$

where α_1, α_2 and α_3 are constants, and l is a length scale. For instance, the GM can be written as

$$\tau_{ij} = G_{u_i u_j} = \frac{\Delta^2}{12}\left[\widetilde{S}_{ik}\widetilde{S}_{kj} - \left(\widetilde{S}_{ik}\widetilde{\Omega}_{kj} - \widetilde{\Omega}_{ik}\widetilde{S}_{kj}\right) - \widetilde{\Omega}_{ik}\widetilde{\Omega}_{kj}\right] \quad (19)$$

It should be noted that the two parts of the GM play different role in SGS modeling. The $\widetilde{S}_{ik}\widetilde{S}_{kj} - \widetilde{\Omega}_{ik}\widetilde{\Omega}_{kj}$ term of the GM is highly aligned with the strain-rate tensor, $\widetilde{S}_{ij}$, and it provides the SGS production of the total SGS energy [21]. The $\widetilde{S}_{ik}\widetilde{\Omega}_{kj} - \widetilde{\Omega}_{ik}\widetilde{S}_{kj}$ term of the GM is highly correlated with the exact SGS stress tensor, while it makes no contribution to the SGS production. To apply the constraint of the indifference of the stress tensor in a frame of reference undergoing rotating, one can modify the GM by removing $\widetilde{\Omega}_{ik}\widetilde{\Omega}_{kj}$. This constraint is perhaps inapplicable to LES if the cutoff of the SGS is not sufficiently small so that the SGS motion could be unaffected by rotation [65]. Thus, the modified GM takes the same format as the nonlinear part of the corrected version of Kosović's model [31]. Therefore, the nonlinear models [31,71,75] discussed in this section are not fundamentally different from mixed structural models.

7 Prospects for the future

This review article has presented an overview of recent efforts aimed at improving parameterizations and making LES a more reliable technique for turbulence studies. We have described the standard eddy-viscosity/diffusivity models and several structural models including models for the SGS stress tensor and the SGS scalar flux vector. A growing body of literature has shown that structural models are important improvements over the standard eddy-viscosity/diffusivity models, especially in the aspect of accurately representing of the energy cascade in the inertial sub-range. Simulation results obtained using structural models help clarify turbulent exchanges, and assist theoreticians and modelers with reliable information about turbulent flows. Several methods, including clipping [38], regularization [2], and mixing [70], facilitate both the stabilization of LESs and the delivery of superior turbulence simulation results. Coefficients obtained using the dynamic procedure have also led to improved predictions. Hence, LESs using structural models have proven themselves to be capable in simulations of high-Reynolds-number turbulent flows that, at present, cannot be resolved by DNS. The outlook for using structural SGS models in turbulence studies is good.

The number of high-quality LES studies is rapidly increasing. LESs can help researchers explore physical behaviors in turbulence, such as the existence of k^{-1} power-law scaling at low wavenumbers in the longitudinal velocity spectrum of wall-bounded turbulence [28]. Meanwhile, the need for accurate simulation has provided much of the impetus for the development of numerical methods in turbulence research. Researchers have examined structural models in LESs of several types of turbulent flows. However, to date, there are relatively few a-posteriori studies involving a consistent set of flow conditions. In closing, future studies should shed light on more comprehensive understanding of SGS models' performances by comparing structural models with classical SGS models in terms of scaling laws [61], space-time correlations in the Eulerian [19,20] and Lagrangian [74,26] frames, higher-order moments in boundary layers [67], and more.

Acknowledgements The contributions of collaborators identified in the cited literature were invaluable in giving content to this article. This material is based upon work supported by the startup funding provided by HUST.

References

1. M. Antonopoulos-Domis. Large-eddy simulation of a passive scalar in isotropic turbulence. *J. Fluid Mech.*, 104:55–79, 1981.
2. G. Balarac, J. L. Sommer, X. Meunier, and A. Vollant. A dynamic regularized gradient model of the subgrid-scale scalar flux for large eddy simulations. *Phys. Fluids*, 25:075107, 2013.
3. S. Banerjee and C. J. Rutland. Study on spray induced turbulence using large eddy simulations. *Atomization and Sprays*, (4):285–316, 2015.
4. J. Bardina, J. H. Ferziger, and W. C. Reynolds. Improved subgrid scale models for large eddy simulation. *AIAA Paper No. 80-1357*, 1980.
5. C. Basdevant and R. Sadourny. Modélisation des échelles virtuelles dans la simulation numérique des éecoulements turbulents bidimensionels. *J. Méc. Théor. Appl., Numéro Spéc.*, pages 243–269, 1983.
6. E. Bou-Zeid, N. Vercauteren, M. B. Parlange, and C. Meneveau. Scale dependence of subgrid-scale model coefficients: an a priori study. *Phys. Fluids*, 20, 2008.
7. C. Cambon, N. N. Mansour, and F. S. Godeferd. Energy transfer in rotating turbulence. *J. Fluid Mech.*, 337:303–332, 1997.

8. W.-C. Cheng and F. Porté-Agel. Evaluation of subgrid-scale models in large-eddy simulation of flow past a two-dimensional block. *Int. J. Heat & Fluid Flow*, 2013.
9. W.-C. Cheng and F. Porté-Agel. Adjustment of turbulent boundary-layer flow to idealized urban surfaces: a large-eddy simulation study. *Boundary-Layer Meteorol.*, 155:249–270, 2015.
10. S. G. Chumakov. Statistics of subgrid-scale stress states in homogeneous isotropic turbulence. *J. Fluid Mech.*, 562:405–414, 2006.
11. S. G. Chumakov and C. J. Rutland. Dynamic structure subgrid-scale models for large eddy simulation. *Int. J. Numer. Meth. Fluids*, 47:911–923, 2005.
12. R. A. Clark, J. H. Ferziger, and W. C. Reynolds. Evaluation of subgrid-scale models using an accurately simulated turbulent flow. *J. Fluid Mech.*, 91(1):1–16, 1979.
13. J. H. Ferziger. Large eddy simulation - a short course. Stanford University, November 2000.
14. M. Gad-el-hak. Fluid mechanics from the beginning to the third millennium. *Int. J. Engng Ed.*, 14(3):177–185, 1998.
15. E. Garnier, N. Adams, and P. Sagaut. *Large eddy simulation for compressible flows*. Springer Netherlands, 2009.
16. M. Germano, U. Piomelli, and W. H. Cabot. A dynamic subgrid-scale eddy viscosity model. *Phys. Fluids A*, 3(7):1760–1765, July 1991.
17. N. S. Ghaisas and S. H. Frankel. A priori evaluation of large eddy simulation subgrid-scale scalar flux models in isotropic passive-scalar and anisotropic buoyancy-driven homogeneous turbulence. *J. Turbul.*, 15(2):88–121, 2014.
18. N. S. Ghaisas and S. H. Frankel. Dynamic gradient models for the sub-grid scale stress tensor and scalar flux vector in large eddy simulation. *J. Turbul.*, 17(1):30–50, 2015.
19. G. W. He, R. Rubinstein, and L. P. Wang. Effects of subgrid-scale modeling on time correlations in large eddy simulation. *Phys. Fluids*, 14(7):2186–2193, 2002.
20. G. W. He, M. Wang, and S. K. Lele. On the computation of space-time correlations by large-eddy simulation. *Phys. Fluids*, 16(11):3859–3867, 2004.
21. K. Horiuti. Roles of non-aligned eigenvectors of strain-rate and subgrid-scale stress tensors in turbulence generation. *J. Fluid Mech.*, 491:65–100, 2003.
22. B. Hu, R. Jhavar, S. Singh, R. D. Reitz, and C. J. Rutland. Combustion modeling of diesel combustion with partially premixed conditions. *SAE Tech. Papers*, (2007-01-0163), 2007.
23. B. Hu, C. J. Rutland, and T. A. Shethaji. A mixed-mode combustion model for large-eddy simulation of diesel engines. *Combust. Sci. and Tech.*, 182:1279–1320, 2010.
24. Y.-N. Huang and H. Lu. Dyadic method for tensor functions. *Acta Mechanica Sinica*, 18(4):398–406, 2002.
25. R. Jhavar and C. J. Rutland. Using large eddy simulations to study mixing effects in early injection diesel engine combustion. *SAE Tech. Papers*, (2006-01-0871), 2006.
26. G. D. Jin, G. W. He, and L. P. Wang. Large-eddy simulation of turbulent collision of heavy particles in isotropic turbulence. *Phys. Fluids*, 22:055106, 2010.
27. Y. Kandea and T. Ishihara. High-resolution direct numerical simulation of turbulence. *J. Turbul.*, 7(20), 2006.
28. G. G. Katul, A. Porporato, and V. Nikora. Existence of k^{-1} power-law scaling in the equilibrium regions of wall-bounded turbulence explained by Heisenberg's eddy viscosity. *Phys. Rev. E*, 86:066311, 2012.
29. W.-W. Kim and S. Menon. A new dynamic one-equation subgrid-scale model for large eddy simulations. *AIAA Paper 1995-356*, 1995.
30. H. Kobayashi and Y. Shimomura. The performance of dynamic subgrid-scale models in the large eddy simulation of rotating homogeneous turbulence. *Phys. Fluids*, 13(8):2350–2360, August 2001.
31. B. Kosović. Subgrid-scale modelling for the large-eddy simulation of high-Reynolds-number boundary layers. *J. Fluid Mech.*, 336:151–182, 1997.
32. D. H. Lenschow, J. C. Wyngaard, and W. T. Pennell. Mean-field and second-moment budgets in a baroclinic, convective boundary layer. *J. Atmos. Sci.*, 37:13131326, 1980.
33. D. K. Lilly. The representation of small-scale turbulence in numerical simulation experiments. *Proc. IBM Sci. Com. Symp. Environmental Sciences (Yorktown Heights, N.Y.)*, page 167, 1967.
34. D. K. Lilly. A proposed modification of the Germano subgrid-scale closure method. *Phys. Fluids*, 4(3):633–635, March 1992.
35. S. Liu, C. Meneveau, and J. Katz. On the properties of similarity subgrid-scale models as deduced from measurements in a turbulent jet. *J. Fluid Mech.*, 275:83–119, 1994.
36. H. Lu. *One-equation LES modeling of rotating turbulence*. Dissertation, University of Wisconsin - Madison, August 2007.
37. H. Lu. Assessment of the modulated gradient model in decaying isotropic turbulence. *Theor. Appl. Mech. Lett.*, 1:041004, 2011.
38. H. Lu and F. Porté-Agel. A modulated gradient model for large-eddy simulation: application to a neutral atmospheric boundary layer. *Phys. Fluids*, 22:015109, 2010.
39. H. Lu and F. Porté-Agel. A modulated gradient model for scalar transport in large-eddy simulation of the atmospheric boundary layer. *Phys. Fluids*, 2013.
40. H. Lu and F. Porté-Agel. On the development of a dynamic non-linear closure for large-eddy simulation of the atmospheric boundary layer. *Boundary-Layer Meteorol.*, 2014.
41. H. Lu and F. Porté-Agel. On the impact of wind farms on a convective atmospheric boundary layer. *Boundary-Layer Meteorol.*, 2015.
42. H. Lu, C. J. Rutland, and L. M. Smith. A priori tests of one-equation LES modeling of rotating turbulence. *J. Turbul.*, 8(37):1–27, 2007.
43. H. Lu, C. J. Rutland, and L. M. Smith. A posteriori tests of one-equation LES modeling of rotating turbulence. *Int. J. Mod. Phys. C*, 19:1949–1964, 2008.
44. T. S. Lund and E. A. Novikov. Parametrization of subgrid-scale stress by the velocity gradient tensor. *Center for Turbulence Research, Annual Research Briefs*, pages 27–43, 1992.
45. P. J. Mason. Large-eddy simulation of the convective atmospheric boundary layer. *J. Atmos. Sci.*, 46(11):1492–1516, 1989.
46. C. Meneveau and J. Katz. Scale-invariance and turbulence models for large-eddy simulation. *Annu. Rev. Fluid Mech.*, 32:1–32, 2000.
47. C.-H. Moeng. A large-eddy-simulation model for the study of planetary boundary-layer turbulence. *J. Atmos. Sci.*, 41:2052–2062, 1984.
48. C.-H. Moeng and R. Rotunno. Vertical-velocity skewness in the buoyancy-driven boundary layer. *J. Atmos. Sci.*, 47:1149–1162, 1990.
49. C.-H. Moeng and J. C. Wyngaard. Spectral analysis of large-eddy simulations of the convective boundary layer. *J. Atmos. Sci.*, 45:3575–3587, 1988.
50. D. Mu noz Esparza, B. Kosović, C. Carcía-Sánchez, and J. Beeck. Nesting turbulence in an offshore convective boundary layer using large-eddy simulations. *Boundary-Layer Meteorol.*, 151:453–478, 2014.
51. U. Piomelli. High Reynolds number calculations using the dynamic subgrid-scale stress model. *Phys. Fluids*, 5:1484–1490, June 1993.
52. U. Piomelli, P. Moin, and J. H. Ferziger. Model consistency in large eddy simulation of turbulent channel flows. *Phys. Fluids*, 31(7):1884–1891, July 1988.

53. U. Piomelli, T. A. Zang, C. G. Speziale, and M. Y. Hussaini. On the large-eddy simulation of transitional wall-bounded flows. *Phys. Fluids A*, 2(3):257–265, February 1990.
54. E. Pomraning and C. J. Rutland. Dynamic one-equation nonviscosity large-eddy simulation model. *AIAA J.*, 40(4):689–701, April 2002.
55. S. B. Pope. *Turbulent flows*. Cambridge University Press, Cambridge, 2000.
56. F. Porté-Agel, C. Meneveau, and M. B. Parlange. A scale-dependent dynamic model for large-eddy simulation: application to a neutral atmospheric boundary layer. *J. Fluid Mech.*, 415:261–284, 2000.
57. C. J. Rutland. Large-eddy simulations for internal combustion engines - a review. *Int. J. Engine Res.*, 12:1–31, 2011.
58. P. Sagaut. *Large eddy simulation for incompressible flows*. Springer-Verlag, Berlin Heidelberg, 3rd edition, 2006.
59. U. Schumann. Subgrid scale model for finite difference simulations of turbulent flows in plane channels and annuli. *J. Comput. Phys.*, 18:376–404, 1975.
60. S. Shamsoddin and F. Porté-Agel. Large eddy simulation of vertical axis wind turbine wakes. *Energies*, 7:890–912, 2014.
61. Z.-S. She and E. Leveque. Universal scaling laws in fully developed turbulence. *Phys. Rev. Lett.*, 72(3):336–339, 1994.
62. J. Smagorinsky. General circulation experiments with the primitive equations: I. the basic experiment. *Mon. Weather Rev.*, 91(3):99–164, 1963.
63. L. M. Smith and F. Waleffe. Transfer of energy to two-dimensional large scales in forced, rotating three-dimensional turbulence. *Phys. Fluids*, 11(6):1608–1622, June 1999.
64. K. Sone and S. Menon. Effect of subgrid modeling on the in-cylinder unsteady mixing process in a direct injection engine. *J. Eng. Gas Turbines Power*, 125(2):435–443, 2003.
65. C. G. Speziale. Subgrid scale stress models for the large-eddy simulation of rotating turbulent flows. *Geophys. Astrophys. Fluid Dynamics*, 33:199–222, 1985.
66. C. G. Speziale. Analytical methods for the development of Reynolds-stress closures in turbulence. *Annu. Rev. Fluid Mech.*, 23:107–157, 1991.
67. R. Stevens, M. Wilczek, and C. Meneveau. Large-eddy simulation study of the logarithmic law for second- and higher-order moments in turbulent wall-bounded flow. *J. Fluid Mech.*, 757:888–907, 2014.
68. C.-W. Tsang, M. F. Trujillo, and C. J. Rutland. Large-eddy simulation of shear flows and high-speed vaporizing liquid fuel sprays. *Computers and Fluids*, 105:262–279, 2014.
69. B. Vreman, B. Geurts, and H. Kuerten. On the formulation of the dynamic mixed subgrid-scale model. *Phys. Fluids*, 6(12):4057–4059, December 1994.
70. B. Vreman, B. Geurts, and H. Kuerten. Large-eddy simulation of the turbulent mixing layer. *J. Fluid Mech.*, 339:357–390, 1997.
71. B.-C. Wang and D. J. Bergstrom. A dynamic nonlinear subgrid-scale stress model. *Phys. Fluids*, 17:035109, 2005.
72. Engine Combustion Network (ECN) website: http://www.sandia.gov/ecn/index.php.
73. J. Wyngaard. *Lectures on air pollution modeling*, chapter "Structure of the PBL". edited by A. Venkatram and J. Wyngaard, American Meteorological Society, Boston, 1988.
74. Y. Yang, G. W. He, and L. P. Wang. Effects of subgrid-scale modeling on Lagrangian statistics in large-eddy simulation. *J. Turbul.*, 9(8):1–24, 2008.
75. Z. Yang, G. Cui, C. Xu, and Z. Zhang. Large eddy simulation of rotating turbulent channel flow with a new dynamic global-coefficient nonlinear subgrid stress model. *J. Turbul.*, 13(48):1–20, 2012.
76. A. Yoshizawa and K. Horiuti. A statistically-derived subgrid-scale kinetic energy model for the large-eddy simulation of turbulent flows. *J. Phys. Soc. Jpn.*, 54(8):2834–2839, August 1985.
77. Y. Zang, R. L. Street, and J. R. Koseff. A dynamic mixed subgrid-scale model and its application to turbulent recirculating flows. *Phys. Fluids A*, 5(12):3186–3196, December 1993.
78. Q.-S. Zheng. Theory of representations for tensor functions - a unified invariant approach to constitutive equations. *Appl. Mech. Rev.*, 47(11):545–587, 1994.